American Journal of Applied Sciences 6 (4): 715-725, 2009
ISSN 1546-9239

Assessment of Surface Treatment on Fatigue Life of Cylinder Block for Linear Engine using Frequency Response Approach

[1]M.M. Rahman, [2]A.K. Ariffin, [2]S. Abdullah, [1]M.M. Noor, [1]Rosli A. Bakar and [3]M. A. Maleque
[1]Automotive Excellence Center, Faculty of Mechanical Engineering,
University Malaysia Pahang, Tun Abdul Razak Highway, 26300 Gambang, Kuantan, Pahang, Malaysia
[2]Department of Mechanical and Materials Engineering, Faculty of Engineering,
University Kebangsaan Malaysia, 43600 UKM, Bangi, Selangor, Malaysia
[3]Faculty of Engineering and Technology,
Multimedia University, Jalan Ayer Keroh Lama, 75450 Bukit Beruang, Melaka, Malaysia

Abstract: **Objectives:** This study was focused on the finite element techniques to investigate the effect of surface treatment on the fatigue life of the vibrating cylinder block for new two-stroke free piston engine using random loading conditions. **Motivation:** An understanding of the effects related to the random loading is necessary to improve the ability of designers to accurately predict the fatigue behavior of the components in service. An internal combustion engine cylinder block is a high volume production component subjected to random loading. **Problem statement:** Proper optimization of this component that is critical to the engine fuel efficiency and more robustly pursued by the automotive industry in recent years. A detailed understanding of the applied loads and resulting stresses under in-service conditions is demanded. **Approach:** The finite element modeling and analysis were performed utilizing the computer aided design and finite element analysis codes respectively. In addition, the fatigue life prediction was carried out using finite element based fatigue analysis code. Aluminum alloys were considered as typical materials in this study. **Results:** The frequency response approach was applied to predict the fatigue life of cylinder block using different load histories. Based on the finite element results, it was observed that the fatigue life was significantly influenced for the nitriding treatment. The obtained results were indicated that the nitrided treatment produces longest life for all loading conditions. **Conclusion:** The nitriding process is one of the promising surface treatments to increase the fatigue life for aluminum alloys linear engine cylinder block.

Key words: Surface treatments, cylinder block, random loading, finite element method, fatigue life, frequency response

INTRODUCTION

Due to market pressures for improvements in productivity, reliability, ductility, wear resistance as well as the profitability of mechanical systems, manufacturers are placing increasing demands on available materials. In order to enhance the surface properties of today's materials, producers of components are turning to different surface treatments[1-2]. There are several techniques available for mechanically improving the surface properties of the components, such as polished, ground, machined, hot rolled, forged, cast, etc. Some of these techniques produce an improve surface by plastic deformation of surface irregularities[3]. Various methods have so far been employed in order to improve fatigue strength, including optimization of geometric design, stronger, materials and surface processing such as nitriding, cold rolled, shot peening, among them shot peening has long been widely used as a low cost and simple method for increasing the fatigue strength of the component.

Light metals have been utilized for automotive parts to reduce the weight of automobiles, aiming at the significant reduction of CO_2 emission and environmental burdens[4-5]. The use of aluminum (Al) instead of steel for lightening of vehicle components or machine parts has recently increased. Al and its alloys have advantages over non metallic materials, aluminum alloys have a high melting point, a good corrosion resistant, a good workability and have a good thermal conductivity. However, the hardness and wear resistance of Al alloys are respectively lower and inferior to those of steel, therefore, there is a limit in their application to moving parts. Hence, research has been carried out in surface modification technology to

Corresponding Author: M.M. Rahman, Automotive Excellence Center, Faculty of Mechanical Engineering,
University Malaysia Pahang, Tun Abdul Razak Highway, 26300 Gambang, Kuantan, Pahang, Malaysia

increase the applicability of Al alloys as moving parts. Surface modification technologies for Al alloys can be classified into three main groups. Alloying is the first method and this forms a hard film on the Al surface[6]. The 2nd group is coating method, which covers the Al surface with hard materials[7]. The third is a heat treating process, such as nitriding[8].The objective of the current study is specifically to investigate into the effect of surface treatments on the fatigue life improvement of the cylinder block of linear engine. Numerical investigates are performed to characterize completely the different induced effects before and after surface treatments. The numerical results were discussed and analyzed. Their influences on HCF behavior of the vibrating component made from AA 6061-T6.

MATERIALS AND METHODS

Theoretical basis of frequency domain: The equation of motion of a linear structural system is expressed in matrix format in Eq. 1. The system of time domain differential equations can be solved directly in the physical coordinate system:

$$[M]\{\ddot{x}(t)\}+[C]\{\dot{x}(t)\}+[K]\{x(t)\}=\{P(t)\} \quad (1)$$

where, {x(t)} is a system displacement vector, [M], [C] and [K] are global mass, damping and stiffness matrices, respectively, {P(t)}is an applied load vector.

When loads are in random in nature, a matrix of the loading power spectral density functions $[S_p(\omega)]$ can be generated by employing Fourier transform of load vector {P(t)}:

$$\left[S_p(\omega)\right]_{m\times m}=\begin{bmatrix} S_{11}(\omega) & \cdots & S_{1m}(\omega) \\ \vdots & \ddots & \vdots \\ S_{m1}(\omega) & \cdots & S_{mm}(\omega) \end{bmatrix} \quad (2)$$

where, m is the number of input loads. The diagonal term $S_{ii}(\omega)$ is the auto-correlation function of load $P_i(t)$and the off-diagonal term $S_{ij}(\omega)$ is the cross-correlation function between loads $P_i(t)$ and $P_j(t)$. From the properties of the cross PSDs, it can be shown that the multiple input PSD matrix $[S_p(\omega)]$ is a Hermitian matrix.

The system of time domain differential equation of motion of the structure in Eq. 1, is then reduced to a system of frequency domain algebra equation:

$$\left[S_x(\omega)\right]_{n\times n}=\left[H(\omega)\right]_{n\times m}\left[S_p(\omega)\right]_{m\times m}\left[H(\omega)\right]^T_{m\times n} \quad (3)$$

where, n is the number of output response variables. The T denotes the transpose of a matrix. $[H(\omega)]$ is the transfer function matrix between the input loadings and output response variables:

$$\left[H(\omega)\right]=\left(-[M]\omega^2+i[C]\omega+[K]\right)^{-1} \quad (4)$$

The response variables $[S_p(\omega)]$ such as displacement, acceleration and stress response in terms of PSD functions are obtained by solving the system of the linear algebra equations in Eq. 3.

Classical FE analysis results in a vector of 6 component stresses at each node. This is shown in Fig. 1. The component stresses consist of 3 normal and 3 shear stress components along the global coordinate or the element coordinate axis and are expressed mathematically in Eq. 5:

$$\begin{aligned} &\text{Normal: } S_{xx}(\omega), S_{yy}(\omega), S_{zz}(\omega) \\ &\text{Shear: } S_{xy}(\omega), S_{yz}(\omega), S_{xz}(\omega) \end{aligned} \quad (5)$$

For the purpose of fatigue analysis a single PSD is required for each node showing some stress equivalent such as von Mises, Tresca or the absolute maximum principal stress. These are obtained by making the eigen values of the stress tensor matrix given by Eq. 6 as follows:

$$\begin{aligned} \sigma_{principal}(\omega) &= \text{eigenvalues}\left(S(\omega)\right) \\ \text{Direction}(\omega) &= \text{eigenvectors}\left(S(\omega)\right) \end{aligned} \quad (6)$$

where, $\sigma_{principal}(\omega)$ is a vector of the three principal stresses, direction (ω) is a matrix of the direction cosines for the three principal axes normalized to yield three unit column vectors, the nth column referring to the nth eigen value. $S(\omega)$ is 3×3 matrix of the component stresses defined as:

$$S(\omega)=\begin{bmatrix} S_{xx}(\omega) & S_{xy}(\omega) & S_{xz}(\omega) \\ S_{xy}(\omega) & S_{yy}(\omega) & S_{yz}(\omega) \\ S_{xz}(\omega) & S_{yz}(\omega) & S_{zz}(\omega) \end{bmatrix} \quad (7)$$

$$\begin{bmatrix} \sigma_1(\omega) \\ \sigma_2(\omega) \\ \sigma_3(\omega) \end{bmatrix} = \text{eigenvelues}\left\{\begin{bmatrix} S_{xx}(\omega) & S_{xy}(\omega) & S_{xz}(\omega) \\ S_{xy}(\omega) & S_{yy}(\omega) & S_{yz}(\omega) \\ S_{xz}(\omega) & S_{yz}(\omega) & S_{zz}(\omega) \end{bmatrix}\right\} \quad (8)$$

The desired stress invariant could be obtained from Eq. 8. The modulus sign is necessary due to the principal stresses returned by Eq. 8 are complex.

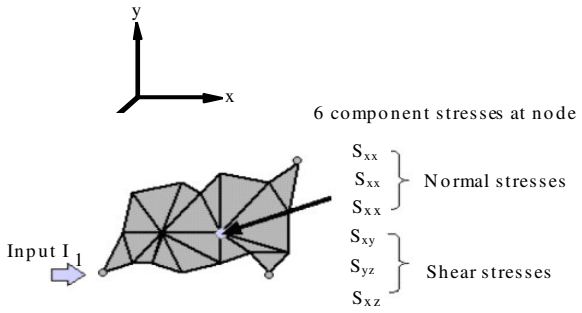

Fig. 1: Transfer function calculated as 6 component stresses

Maximum principal stress:

$$\sigma_{max}(\omega) = \max\left(\left|\sigma_1(\omega)\right|,\left|\sigma_2(\omega)\right|,\left|\sigma_3(\omega)\right|\right) \quad (9)$$

Von Mises stress:

$$\sigma_{von\ Mises}(\omega) = \sqrt{\frac{1}{2}\cdot\left(\left|\sigma_1(\omega)-\sigma_2(\omega)\right|^2+\left|\sigma_2(\omega)-\sigma_3(\omega)\right|^2+\left|\sigma_3(\omega)-\sigma_1(\omega)\right|^2\right)} \quad (10)$$

Tresca:

$$\sigma_{Tresca}(\omega) = \max\begin{pmatrix}\left|\sigma_1(\omega)-\sigma_2(\omega)\right|,\ \left|\sigma_2(\omega)-\sigma_3(\omega)\right|,\\ \left|\sigma_3(\omega)-\sigma_1(\omega)\right|\end{pmatrix} \quad (11)$$

where, $\sigma_{xxx}(\omega)$ is the transfer function with respect to frequency (ω) rad/sec expressed as a stress invariant. Frequency can also be expressed in terms of Hz after using the appropriate conversion.

Frequency response methods: This research was described variety of approaches for computing fatigue life or damage directly from the PSD of stress as opposed to a time history. The stress power spectra density represents the frequency domain approach input into the fatigue[9]. This is a scalar function that describes how the power of the time signal is distributed among frequencies. Mathematically this function can be obtained by using a Fourier Transform of the stress time history auto-correlation function and its area represents the signals standard deviation. It is clear that PSD is the most complete and concise representation of a random process.

Bendat presented the theoretical basis for the first of these of these frequency domain fatigue models, so called Narrow band solution. This expression was defined solely in terms of the spectral moments up to m_4.

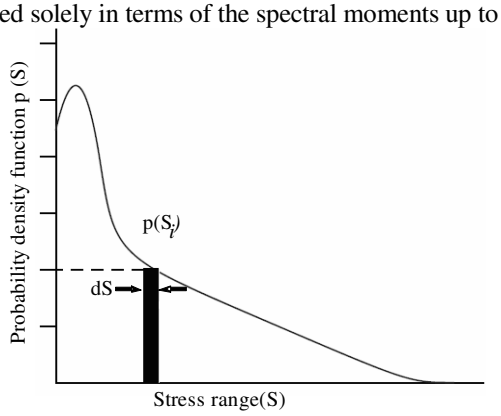

Fig. 2: Probability density functions

However, the fact that this solution was suitable only for a specific class of response conditions was an unhelpful limitation for the practical engineer. Bendat showed that the probability density function of peaks for a narrow band signal tended towards Rayleigh distributions as the bandwidth reduced. To complete his solution method, Bendat used a series of equations derived by Rice [10] to estimate the expected number of peaks using moments of area beneath the PSD.

The most convenient way of storing stress range histogram information is in the form of a Probability Density Function (PDF) of stress ranges. A typical representation of this function is shown in Fig. 2. It is easily to transform from a stress range histogram to a PDF, or back to time histories. The bin widths used and the total number of cycles recorded in the histogram are the only additional information required. To get a PDF from a rainflow histogram each bin in the rainflow count has to be multiplied by $S_t$xdS, where S_t is the total number of cycles in histogram and dS is the interval width. The probability of the stress range occurring between S_i-dS/2 and S_i+dS/2 is given by $p(S_i)dS$.

The actual counted number of cycles, $n_i = p(S)\,dSS_t$:

The allowable number of cycles: $$N(S_i)=\frac{k}{S^b} \quad (12)$$

Assume p(S) is the Rayleigh distribution which s represented by a narrow band process and stress amplitude, S, can be treated as a continuous random variable.

$$p(S)_{NB} = f(m_0) = \frac{S}{4m_0}e^{\frac{-S^2}{8m_0}} \quad (13)$$

The expected total fatigue damage for narrow band gaussian process:

$$E[D]=\sum_i \frac{n_i}{N(S_i)}=\frac{S_t}{K}\int S^b\ p(S)\,dS$$
$$=\frac{E[P]T}{K}\int S^b\left[\frac{S}{4\,m_0}\ e^{\frac{-S^2}{8m_0}}\right]dS \quad (14)$$

where, $N(S_i)$ is the number of cycles of stress range S occurring in T sec, n_i is the actual counted number of cycle, S_t is the total number of cycles equals to $E^{[P]}T$. Failure occurs, D≥ 1.0.

In order to compute fatigue damage over the lifetime of the structure in secpnd, the form of materials S-N data must also be defined using the material parameters k and b. The typical S-N curve for high cycle fatigue is as shown in Fig. 3.

Figure 3 shows that, under constant amplitude cyclic loading, a linear relationship exists between cycles to failure (N) and applied stress range (S) when plotted on log-log study. There are two alternative ways of defining this relationship, as given in Eq. 15:

$$N=kS^{-b},\ \text{where}\ b=-\frac{1}{b1}\ \text{and}\ k=(SRI1)^b \quad (15)$$

A method for computing PSD moments is described by Rahman. Some very important statistical parameters can be computed from these moments. These parameters are Root Mean Square (RMS), number of Zero crossing with positive slope (E[0]), number of peaks per second (E[P]). The formulas in Eq. 16 highlight these properties of the spectral moments:

$$RMS=\sqrt{m_0}\ ;\qquad E[0]=\sqrt{\frac{m_2}{m_0}};\qquad E[P]=\sqrt{\frac{m_4}{m_2}} \quad (16)$$

where, m_0, m_1, $m_2$and m_4 are the zero, 1st, 2nd and 4th order moment of area of the PSD respectively.

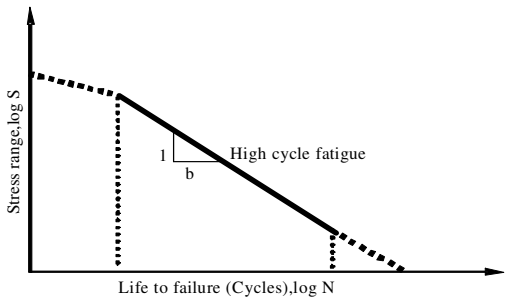

Fig. 3: Typical S-N curve for high cycle fatigue

Another important property of spectral moments is the fact that it is possible to express the irregularity factor as a function of the zero, 2nd and 4th order spectral moments, as expressed in Eq. 17:

$$\gamma=\frac{E[0]}{E[P]}=\frac{m_2}{\sqrt{m_0 m_4}} \quad (17)$$

Figure 4 shows how to calculate the irregularity factor. When irregularity factor is equal to 0, there are an infinite number of peaks for every zero up crossing. This is considered a wide band random process. The value of irregularity factor is equal to 1 corresponds to one peak per one zero up crossing and it represents a narrow-band random process. Alternatively, a narrow-band process can be defined by the width of its spectrum. For this reason, the spectral width parameter, λ, is introduced as Eq. 18:

$$\lambda=\sqrt{1-\gamma^2} \quad (18)$$

That means λ = 0 represents a narrow-band random process.

The irregularity factor γ is an important parameter that can be used to evaluate the concentration of the process near a central frequency. Therefore, the irregularity factor can be used to determinate whether the process is narrow band or wide band. Irregularity factor varies between 1 and 0. A narrow band process (γ→1) is characterized by only one predominant central frequency indicating that the number of peaks per second is very similar to the number of zero crossings of the signal. This assumption leads to the fact that the PDF of the fatigue cycles range is the same as the PDF of the peaks in the signal. In this case fatigue life is easy to estimate.

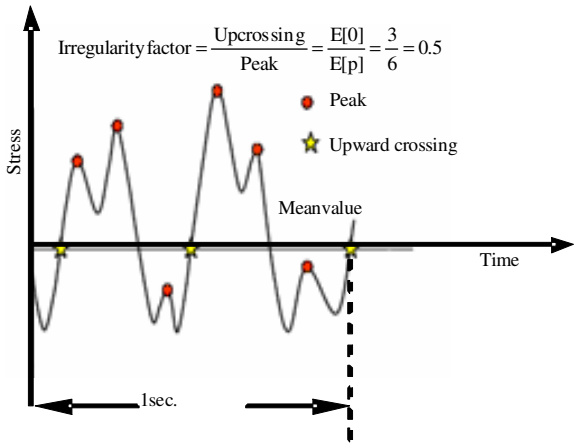

Fig. 4: Calculation of the irregular factor, γ

Many expressions have been proposed to correct the conservatism associated with this solution. The solutions of Wirsching and Light[11], Tunna[12], Chaudhury and Dover[13], Steinberg[14], and Hancock[15] were all derived using this approach. They are all expressed in terms of the spectral moments up to m_4.

Tunna solution:

$$p(S)_T = \left[\frac{S}{4\gamma m_0} e^{-\frac{-S^2}{8\gamma m_0}} \right] \quad (19)$$

Wirsching solution:

$$E[D]_{Wirsching} = E[D]_{NB} \left[a + [1-a](1-\varepsilon)^c \right] \quad (20)$$

Where:

$$\varepsilon = \sqrt{1-\gamma^2}$$

where, ε is a spectral bandwidth parameter which is an alternative version of the irregularity factorand a and c are best fitting parameters expressed as:

$$a = 0.926 - 0.033b; c = 1.587b - 2.323 \quad (21)$$

where, b is the slope of the S-N curves which is defined in Eq. 15.

This solution is given in the form of an equivalent stress range parameter S_{eq},

Where:

$$S_{eq} = \left[\int_0^\infty S^b \, p(S) \, dS \right]^{\frac{1}{b}} \quad (22)$$

Hancock equivalent stress:

$$(S_{eq})_{Hancock} = \left(2\sqrt{2\, m_0}\right) \left[\gamma \Gamma\left(\frac{b}{2}+1\right) \right]^{\frac{1}{b}} \quad (23)$$

Chaudhury and dover equivalent stress:

$$(S_{eq})_{C\&D} = \left(2\sqrt{2\, m_0}\right) \left[\begin{array}{l} \frac{\varepsilon^{b+2}}{2\sqrt{\pi}} \Gamma\left(\frac{b+1}{2}\right) + \frac{\gamma}{2} \Gamma\left(\frac{b+2}{2}\right) \\ + \text{erf}^*(\gamma) \frac{\gamma}{2} \Gamma\left(\frac{b+2}{2}\right) \end{array} \right]^{\frac{1}{b}} \quad (24)$$

Where:

$$\text{erf}^*(\gamma) = 0.3012\gamma + 0.4916\gamma^2 + 0.9181\gamma^3 - 2.354\gamma^4 - 3.3307\gamma^5 + 15.6524\gamma^6 - 10.7846\gamma^7$$

Steinberg Solution:

$$(S_{eq})_{Steinberg} = \left[\begin{array}{l} 0.683 \left(2\sqrt{m_0}\right)^b \\ + 0.271 \left(4\sqrt{m_0}\right)^b - 0.043 \left(6\sqrt{m_0}\right)^b \end{array} \right]^{\frac{1}{b}} \quad (25)$$

The fatigue damage can then easily be obtained by substituting this into the general damage equation used when deriving the narrow band solution:

$$E[D] = \frac{E[P]\, T}{k} S_{eq} \quad (26)$$

Probably the most famous empirical formula for approximating the rain flow amplitude distribution is that proposed by Dirlik, which uses a combination of an exponential and two Rayleigh densities. In the Dirlik model, approximate closed-form expression for the probability density function of rain flow ranges, which was obtained using Monte Carlo technique. The Dirlik solution is expressed by the Eq. 27 and details the specific literature reported in the refs[16-17]:

$$N(S) = E[P]\, T\, p(S) \quad (27)$$

where, N(S) is the number of stress cycles of range S (N/mm^2) expected in T seconds, $E^{[P]}$ is the expected number of peaks and p(S) is the probability density function:

$$p(S) = \frac{\frac{D_1}{Q} e^{\frac{-Z}{Q}} + \frac{D_2 Z}{R^2} e^{\frac{-Z^2}{2R^2}} + D_3 Z e^{\frac{-Z^2}{2}}}{2\sqrt{m_0}} \quad (28)$$

where, p(S) is the probability density function, S is the stress amplitude, m_0 is the zeroth order spectral moment and:

$$\gamma = \frac{m_2}{\sqrt{m_0\, m_4}}, \; x_m = \frac{m_1}{m_0}\sqrt{\frac{m_2}{m_4}}, \; D_1 = \frac{2(x_m - \gamma^2)}{1+\gamma^2}$$

$$R = \frac{\gamma - x_m - D_1^2}{1-\gamma-D_1+D_1^2}, \; Z = \frac{S}{2\sqrt{m_0}}, \; D_2 = \frac{1-\gamma-D_1+D_1^2}{1-R}$$

$$D_3 = 1 - D_1 - D_2, \; Q = \frac{1.25(\gamma - D_3 - D_2 R)}{D_1}$$

where, x_m, D_1, D_2, D_3, Q, Z and R parameters depending on the m_0, m_1, m_2 and m_4, Z is a normalized variable. m_0, m_1, m_2 and m_4 are the zeroth, 1st, 2nd and 4th order spectral moments, respectively. It should be noted that, if compared to the Wirsching-Light model, this approach gives an amplitude distribution (and thus a rain flow damage) depending on just four spectral moments (i.e. m_0, m_1, m_2 and m_4), including in particular a dependence on m_1 moment. All of above discussed methods are determining fatigue life from PSDs stress.

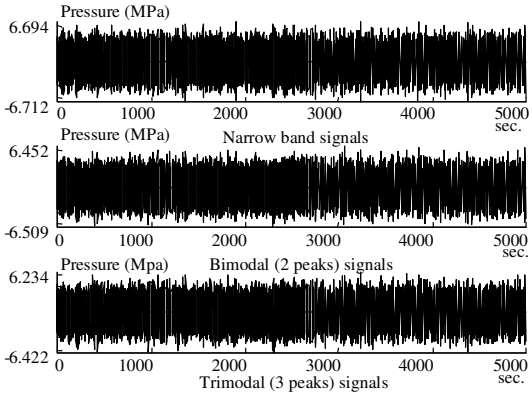

Fig. 5: Time-loading histories of narrow band, bimodal and trimodal signals

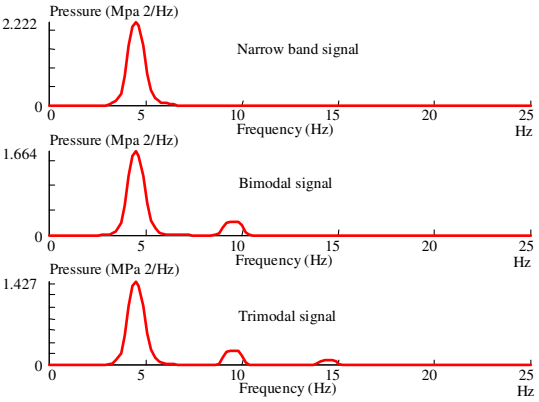

Fig. 6: Power spectral density functions of the narrow band, bimodal and trimodal signals

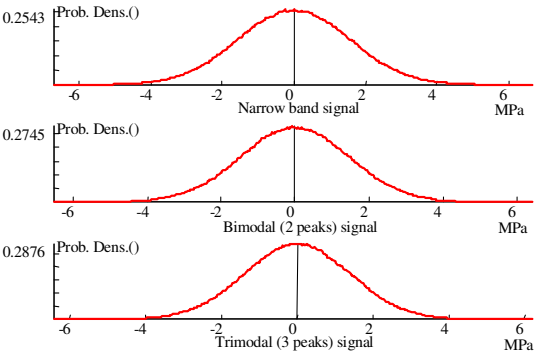

Fig. 7: Probability density functions of the narrow band, bimodal and trimodal signals

Loading information: Figure 5 shows the time-load histories signals of the narrow band (1 peak) and two wide band of bimodal (2 peaks) and trimodal (3 peaks) loading histories[18]. Figure 6 and 7 also show the power spectral density function and corresponding probability density function of those signals.

RESULTS AND DISCUSSION

A geometric model of the cylinder block of the free piston engine is considered in this study. Three-dimensional model geometry was developed in CATIA® software. Since the tetrahedral is found to be the best meshing technique, the 4 nodes tetrahedral (TET4) element version of the cylinder block was used for the initial analysis. In addition, the TET4 compared to the 10 nodes tetrahedral (TET10) element mesh using the same global mesh length for the highest loading conditions (7.0 MPa) in the combustion chamber. The investigating the results, it can be found that the TET10 mesh predicted higher von Mises stresses than that the TET4 mesh. The TET10 mesh is presumed to represent a more accurate solution since TET4 meshes are known to be dreadfully stiff[19]. TET4 employed a linear order interpolation function while TET10 used quadratic order interpolation function. For the same element size, the TET10 is expected to be able to capture the high stress concentration associated with the bolt holes. A TET10 was then finally used for the solid mesh. Mesh study is performed on the FE model to ensure sufficiently fine sizes are employed for accuracy of calculated results but at competitive cost (CPU time). In the process, specific field variable is selected and its convergence is monitored and evaluated. Sensitivity analysis was performed to obtain the optimum element size. The analysis was performed iteratively at different element lengths until the solution obtained appropriate accuracy. Convergence of the stresses was observed, as the mesh size was successively refined. The element size of 0.20 mm was finally considered. A total of 35415 elements and 66209 nodes were generated with 0.20 mm element length. Compressive loads were applied as pressure (7 MPa) acting on the surface of the combustion chamber and preloads were applied as pressure (0.3 MPa) acting on

the bolt-hole surfaces. In addition, preload was also applied on the gasket surface generating pressure of 0.3 MPa. The loading and constraints on the cylinder block are shown in Fig. 8. The constraints were applied on the bolt-hole for all six degree of freedoms.

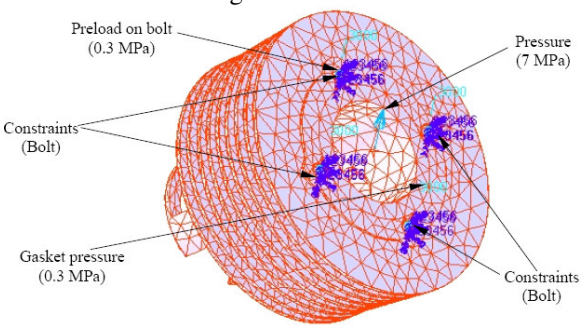

Fig. 8: Loading and constraints on the cylinder block

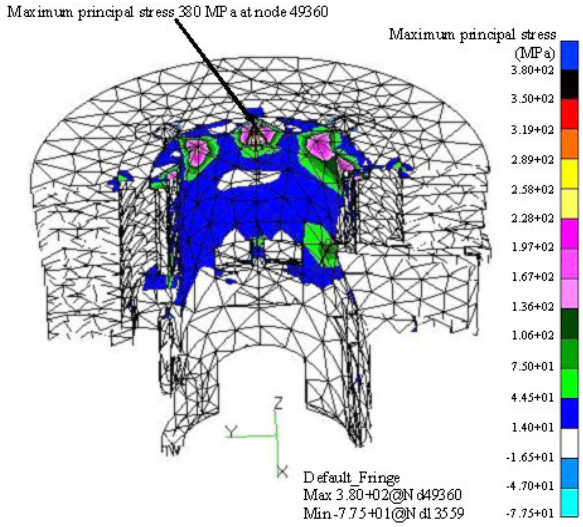

Fig. 9: Maximum principal stresses distribution for the Pseudo-static linear analysis

The finite element results of time domain (Pseudo-static method) i.e., the maximum principal stresses distribution is shown in Fig. 9. The fatigue life of time domain histories are performed using the stress-life method employed rain flow cycle counting technique[20-21]. Time domain fatigue approach consists of a number of steps. The first is to count the number of stress cycles in the response time history. This is performed through a process of rain flow cycle counting. Damage from each cycle is determined, typically from an S-N curve. The damage is then summed over all cycles using linear damage summation techniques to determine the total life. The frequency response analyses were performed using the finite element analysis code. The frequency response analysis used the damping ratio of (5%) of critical. The damping ratio is the ratio of the actual damping in the system to the critical damping. Most of the experimental modal

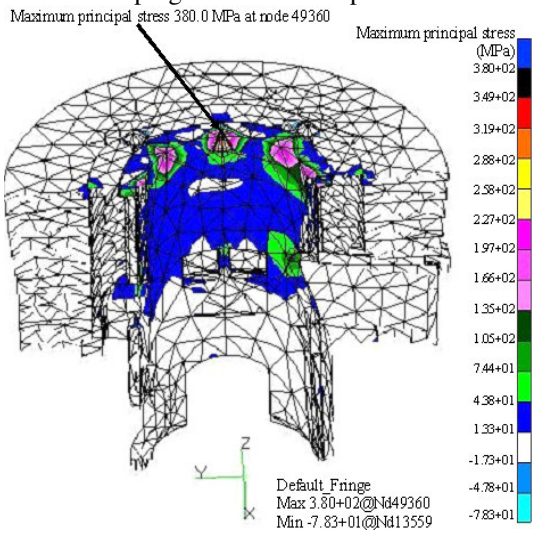

Fig. 10: Maximum principal stresses distribution for the frequency response analysis with zero Hz

reported that the modal damping in terms of non-dimensional critical damping ratio expressed as a percentage[22-23]. In fact, most structures have critical damping values in the range of (0-10%), with values of (1-5%) as the typical range. Zero damping ratio indicates that the mode is un damped. Damping ratio of one represents the critically damped mode. The result of the frequency response finite element analysis with zero Hz i.e. the maximum principal stresses distribution of the cylinder block is shown in Fig. 10. From the results, the maximum and minimum principal stresses of 380.0 and -77.5 MPa for the Pseudo static analysis and 380.0 and -78.3 MPa for the frequency response analysis for zero Hz were obtained respectively. These two maximum principal stresses contour plots are almost identical.

The variation of the maximum principal stresses with the frequency is shown in Fig. 11. It can be seen that the maximum principal stress varies with the higher frequencies. This variation is due to the dynamic influences of the first mode shape. It is also observed that the maximum principal stress occurs at a frequency of 32 Hz. The maximum principal stresses of the cylinder block for 32 Hz is shown in Fig. 12. From the results, the maximum and minimum principal stresses of 561.0 and -207.0 MPa were obtained at node 49360 and 47782 respectively.

The results of the fatigue life contour for the narrow band loading histories at most critical locations for Pseudo-static analysis and frequency response approach with 32 Hz are shown in Figure 13 and 14 respectively. The minimum life prediction for Pseudo-static analysis and frequency response approach with 32 Hz are obtained $10^{7.67}$ and $10^{9.44}$ sec respectively.

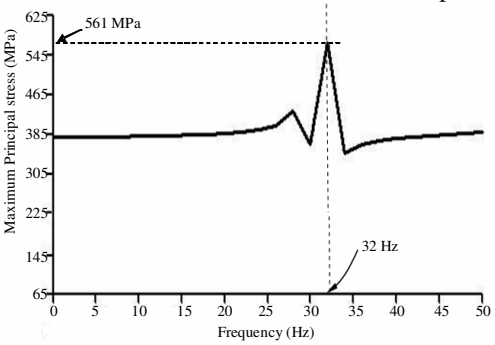

Fig. 11: Maximum principal stresses plotted against frequency

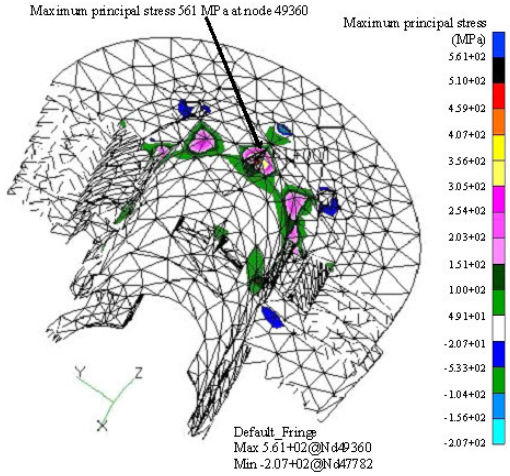

Fig. 12: Maximum principal stresses contour for the frequency response analysis with 32 Hz

It would be expected that the condition of lower stress would correspond to longer life and vice versa. However, the results indicates the opposite because the frequency resolution of the transfer function are selected the small value then the result show the non-conservative prediction. From Figure 13 and 14, it can be seen that the fatigue life contours are different and most damage was found at frequency of 32 Hz. The predicted fatigue life on log-log coordinates using the Pseudo-static and the frequency response analysis is shown in Fig. 15. The dotted straight line on the Fig. 15 shows the perfect correlation between the Pseudo-static and frequency response approach. It can be seen that the predicted results are well correlated between these approaches.

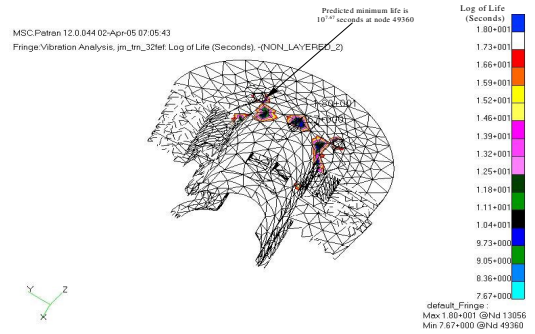

Fig. 13: Predicted fatigue life contours plotted for Pseudo-static analysis

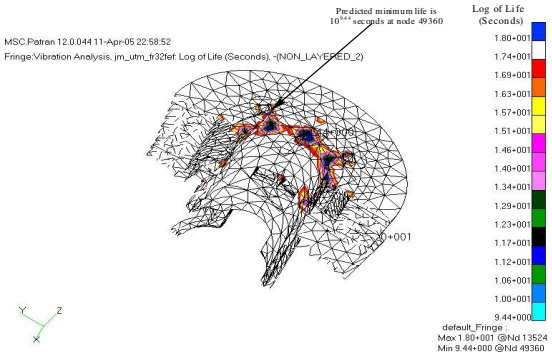

Fig. 14: Predicted fatigue life contours plotted for the frequency response analysis with 32 Hz

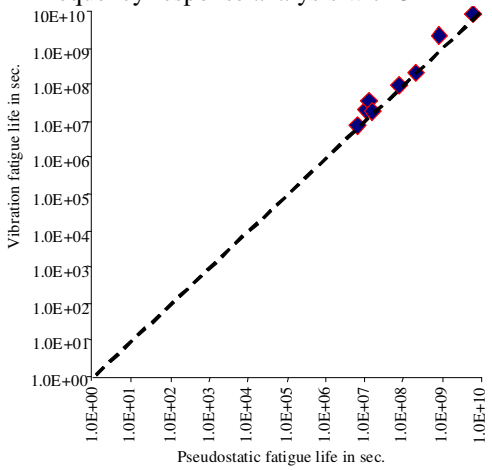

Fig. 15: Comparison between the fatigue life of the Pseudo-static and the frequency response analysis

Effect of frequency resolution: Frequency resolution of the transfer function is significant to capture the input PSD. The significances of the frequency resolutions of SAEBKT loading histories are also shown in Fig. 16 and 17. Two types of Fast Fourier Transform (FFT) buffer size width namely 8192:0.06104 Hz and 16384:0.03052 Hz were used in Fig. 16 and 17. The FFT buffer size defines the resolution of the power spectrum. The buffer must be a power of 2 and of course the longer the buffer, the higher the resolution of the spectral lines. To calculate the resolution divide the Nyquist frequency by half the FFT buffer size. If the Nyquist frequency is 250 Hz and the FFT buffer size selected is 8192, then the spectral lines are 250/(8192/2) = 0.06104 Hz apart. Another use of a smaller buffer size is for short data files as these cannot be adequately analyzed with a big buffer, since there may not be enough data to give a good spectral average. Using a smaller buffer size could give a better spectral average at the expense of spectral line width. The total area under each input PSD curve is determined to be identical. However, the 16384:0.03052 Hz width has twice as many points compares to the 8192:0.06104 Hz.

Table 1 is shown the comparison between the narrow band (1 peak) and wide band of bimodal (2 peaks) and trimodal (3 peaks) loading histories with the time domain from all the frequency domain approach methods. From the results, it can be seen that the Dirlik method gives the best results for all three loading conditions (narrow band and wide band signals). The narrow band gives good results from the narrow band signal (1 peak), but becomes too conservative when the signal is bimodal and trimodal signals (2 and 3 peaks). Tunna breaks down completely for a wide band signal. Wirsching is non conservative and then too conservative as is Steinberg. Hancock, Chaudhury and Dover do reasonably well but not as well as Dirlik model. When the signal is wide band (bimodal and trimodal), the narrow band tends to turn any signal into a narrow band signal making the resulting prediction fatigue life extremely and sometimes overly conservative. The Dirlik method found to gives the best results when compared with the corresponding time domain result and others. From the above discussions, it is concluded that the Dirlik method is recommended for general usage.

Effect of surface treatments: The investigation of the effect of surface treatments on the fatigue life of component subjected to random loading conditions. The material used in this study is AA6061-T6. Power spectral density with FFT buffer size 16384:0.03052 Hz width are consider in this analysis. A high proportion of all fatigue failures nucleate at the surface of components and thus surface conditions become an extremely important factor influencing fatigue strength.

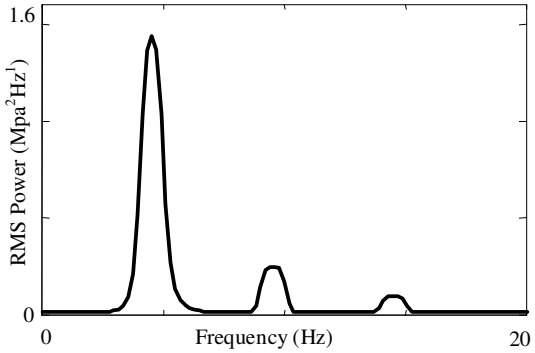

Fig. 16: Power spectral density when using the FFT buffer size of 8192:0.06104 Hz width

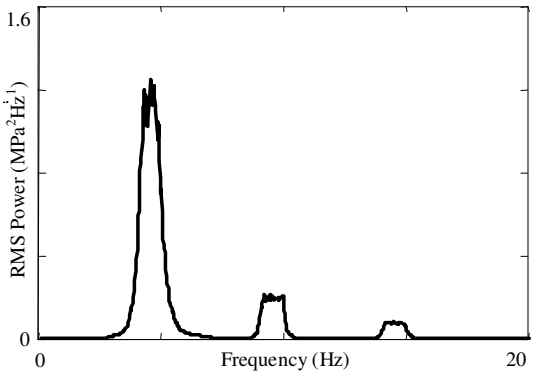

Fig. 17: Power spectral density when using the FFT buffer size of 16384:0.03052 Hz width

Table 1: Predicted fatigue life at critical location (Node 49360) for various frequency response approaches using the narrow and wide band signal

Load-time histories signals	Predicted Fatigue life at critical location in sec (10^6)							
	Time domain	Narrow band	Dirlik	Tunna	Wirsching	Hancock	Chaudhury and dover	Steinberg
Narrow band	2.66	2.61	2.65	5.83	3.83	2.47	2.46	3.18
Bimodal	4.48	2.49	4.30	1.11	4.23	3.81	4.53	3.51
Trimodal	6.16	2.55	6.38	3.79	4.32	5.19	7.46	3.67

Table 2: The effect of the surface finish and treatments on the fatigue life at critical location (node 49360) for 3 peaks loading conditions

Surface finish processes	Predicted vibration fatigue life in years			
	Untreated	Shot peened	Cold rolled	Nitrided
Polished	0.202	0.644	10.430	808.600
Ground	0.104	0.425	0.104	170.600
Good machined	0.063	0.450	6.532	54.540
Poor machined	0.026	0.149	1.475	8.689
Forged	0.010	1.265	0.010	1.265
Cast	0.009	0.064	0.009	1.091

Surface effects are caused by differences in surface roughness, microstructure, chemical composition and residual stress. The correction factor for surface finish is sometimes used a qualitative description of surface finish such as polished or machined. The surface factors as a function of ultimate tensile strength involving different surface finish conditions such as grinding, machining, hot rolling and as-forged. The correction factors for surface treatment and finish are obtained from the empirical data and are related to the ultimate strength of the material.

The comparison between the surface treatments with various surface finish processes using the 3 peaks wide band signal time-loading histories are shown in Table 2. It can be seen that the fatigue life for nitriding surface treatments is surprisingly increases than those other surface treatment processes due to the development of compressive residual stresses and the increase of hardness near the surface. It can be shown in Table 2 that there are no effect on ground, forged and cast surface finish condition with the cold rolled surface treatments. Forging can cause surface decarburization and the loss of carbon atoms from the surface material causes it to have a lower strength and may also produce residual tensile stresses. Both of these factors are especially detrimental to fatigue strength.

Surface treatments including nitriding, cold rolling and shot peening that produced compressive residual surface stresses can prolong the fatigue life. These surface treatments cause the maximum tensile stress to occur below the surface of the materials. However, the tensile residual surface stresses are found to be especially detrimental and can promote corrosion fatigue. In addition, Surface treatments can also increase the endurance limit of the material used. A diffusion process such as nitriding is found to be a dreadfully beneficial for increasing the fatigue strength. This process is capable of increasing the strength of the material on the surface as well as causing the volumetric changes, which produce the residual compressive surface stresses. Thus the nitriding could be applied to the fatigue critical area of the subject to improve the fatigue life and also improve the fretting resistance, since the cylinder block is in contact with other components.

CONCLUSION

This study was conveyed the important findings on the influence of the surface treatment process parameter on the fatigue lives. Frequency domain fatigue analysis was applied to a typical cylinder block of two-stroke free piston engine. The results show that all surface treatment processes can be applied to increase the fatigue life of the aluminum alloys component. The surface compressive residual stress was the greatest effect on the fatigue life. According to the results, it was concluded that the polished and nitriding combinations found the great influences on the fatigue life improvement. Nitriding treatment was to produce compressive forces in the outer layers of the component. The compressive residual stresses and the tensile residual stresses found to be beneficial and detrimental to the fatigue life respectively. The nitriding process has the combined effect of producing a higher material strength on the surface and causing the volumetric changes which produce the residual compressive stresses. In addition, the vibration fatigue analysis be capable of improve understanding of the system behaviors in terms of frequency characteristics of both structures and loads and their couplings.

ACKNOWLEDGEMENT

The researchers would like to thank the Department of Mechanical and Materials Engineering, Faculty of Engineering, Universiti Kebangsaan Malaysia to provided the laboratory facilities. The authors would like to express their especial thanks to Universiti Malaysia Pahang for provided financial support.

REFERENCES

1. Rahman, M.M., A.K. Ariffin, S. Abdullah and A.B. Rosli, 2007. Effect of nitriding treatment on fatigue life for free piston linear engine component using frequency response method: A finite element approach. Struct. Durabil. Hum. Monitor., 3: 197-210. http://www.techscience.com/paper.asp?jnl=sdhm&issue=v3n4&no=15
2. Rahman, M.M., A.K. Ariffin, N. Jamaludin and C.H.C. Haron, 2006. Influence of surface treatments on fatigue life of a free piston linear generator engine component using random loading. J. Zhejiang Univ. Sci. A., 7: 1819-1830. DOI: 10.1631/jzus.2006.A1819

3. Rahman, M.M. and A.K. Ariffin, 2006. Effects of surface finish and treatment on the fatigue behaviour of vibrating cylinder block using frequency response approach. J. Zhejiang Univ. Sci. A., 7: 352-360. DOI: 10.1631/jzus.2006.A0352
4. Rahman, M.M., A.K. Ariffin, N. Jamaludin and C.H.C. Haron, 2006. Influence of surface treatments on fatigue life of a free piston linear generator engine component using Narrow band approach. Struct. Durabil. Health Monitor., 2: 69-82. http://www.techscience.com/paper.asp?jnl=sdhm&issue=v2n2&no=06
5. Boms, R. and D. Whitacre, 2005. Optimization design of aluminum suspension components using an integrated approach. SAE Technical Paper no. 2005-01-1387. http://www.sae.org/technical/papers/2005-01-1387
6. Okumiya, M., Y. Tsunekawa, H. Sugiyama, Y. Tanaka, N. Takano and M. Tomimoto, 2005. Surface modification of aluminum using ion nitriding and barrel nitriding. Surf. Coat. Technol., 200: 35-39. DOI: 10.1016/j.surfcoat.2005.02.110
7. Tsunekawa, Y., T. Ueno, M. Okumiya and T. Yashiro, 2003. Plasma sprayed coating with water and gas atomized steel powders. Surf. Eng., 19: 17-22. DOI: 10.1179/026708402225010074
8. Tomida, S. and K. Nakata, 2003. Fe-Al composite layers on aluminum alloy formed by laser surface alloying with ion powder. Surf. Coat. Technol., 174-175: 559-563. DOI: 10.1016/S02578972(03)00698-4.
9. Bishop, N.W.M. and F. Sherratt, 2000. Finite Element Based Fatigue Calculations. 1st Edn., NAFEMS Ltd., Scotland, UK. http://www.nafems.org/publications/
10. Rice, S.O., 2000. Mathematical analysis of random noise- and appendixes. Technical Publications, Bell Telephone Labs, Inc., New York, USA., pp. 1-162. http://handle.dtic.mil/100.2/ADB802399
11. Wirsching, P.H. and C.L. Light, 1980. Fatigue under wide band random stresses. J. Struct. Div., ASCE., 106: 1593-1607. http://cedb.asce.org/cgi/WWWdisplay.cgi?5015574
12. Tunna, J.M. 1986. Fatigue life prediction for Gaussian random loads at the design stage. Fat. Frac. Eng. Mat. Struct., 9: 169-184. DOI: 10.1111/j.1460-2695.1986.tb00444.x
13. Chaudhury, G.K. and W.D. Dover, 1985. Fatigue analysis of offshore platforms subjected to sea wave loading. Int. J. Fatigue, 7: 13-19. DOI: 10.1016/0142-1123(85)90003-9
14. Van Hulle, F.J., 1991. Wind energy: Technology and implementation. Proceeding of the European Conference on EW, Oct. 14-18, Amsterdam, The Netherlands, pp: 246-250. ISBN: 044489117X.
15. Kam, J.C.P. and W.D. Dover, 1988. Fast fatigue assessment procedure for offshore structures under random stress history. ICE Proc. Lond., 85: 689-700. DOI: 10.1680/iicep.1988.951
16. Fu, T.T. and D. Cebon, 2000. Predicting fatigue lives for bimodal stress spectral densities. Int. J. Fatigue, 22: 11-21. DOI: 10.1016/S0142-1123(99)00113-9
17. Haiba, M., D.C. Barton, P.C. Brooks and M.C. Levesley, 2002. Review of life assessment techniques applied to dynamically loaded automotive components. Comput. Struct., 80: 481-494. DOI: 10.1016/S0045-7949(02)00022-6
18. Bishop, N.W.M. and F. Sherratt, 1989. Fatigue life prediction from power spectral density data. Part-1, Traditional approaches and part-2 recent developments. Environ. Eng., 2: 11-19. http://connection.ebscohost.com/content/article/1024619187.html
19. Felippa, C.A., 2008. Advanced Finite Element Methods. http://caswww.colorado.edu/courses.d/AFM.d/Home.html
20. Anthes, R.J. 1997. Modified rainflow counting keeping the load sequence. Int. J. Fatigue, 19: 529-535. DOI: 10.1016/S0142-1123(97)00078-9
21. Khosrovaneh, A.K. and N.E. Downing, 1990. Fatigue loading history reconstruction based on rainflow technique. Int. J. Fatigue, 12: 90-106. DOI: 10.1016/0142-1123(90)90679-9
22. Formenti, D. 1999. The relationship between % of critical and actual damping in a structure. Sound Vibrat., 33: 14-18. http://www.sagetechnologies.com/library_documents/dave_qa/q&aapr9.pdf
23. Gade, S., H. Herlufsen and H. Konstantin-Hansen, 2002. How to determine the modal parameters of simple structures. Sound Vibrat., 36: 72-73. http://www.bksv.com/doc/Bo0428.pdf